

# DETECTION OF SMALL AIRCRAFT WITH DOPPLER WEATHER RADAR

Svetlana Bachmann<sup>1,2</sup>, Victor DeBrunner<sup>3</sup>, Dusan Zrnic<sup>2</sup>

<sup>1</sup> Cooperative Institute for Mesoscale Meteorological Studies, The University of Oklahoma

<sup>2</sup> National Severe Storm Laboratory, NOAA/OAR

<sup>3</sup> Florida State University

## ABSTRACT

We present a method that can be performed in parallel to reflectivity estimation in weather radar and that allows one to detect small aircraft. Though small aircraft and large birds might produce comparable reflectivity signals their spectral signatures are considerably different. A small aircraft with propellers can be recognized from its spectrum via modulations produced by Doppler shifts from rotating parts. Generally such a spectrum has an elevated spectral floor compared to the spectrum of a resolution volume without an airplane. The spectral floor level is used for detection. The method is demonstrated on a clear air case observed with Doppler weather radar on March 6, 2007 at elevation 0.5°.

**Index Terms** — frequency domain analysis, noise measurement, adaptive signal processing.

## 1. INTRODUCTION

The National Weather Service's network of Doppler Weather Radars (WSR-88D) covers the entire US. The main purpose of the network is weather observation and quantitative precipitation measurement. These radars operate continuously and each covers a spatial volume in about five minutes. In clear air conditions, radars perform wind profile estimations. The work load on the radars in clear air can be increased by such application that would detect and track aircraft without compromising radars' primary mission objectives.

Weather radar is capable of detecting echoes from a small aircraft or from a large bird. However, there is no direct way to categorize these detected echoes. Rapid consecutive scans are required to track the echo, evaluate its velocity and determine if it is indeed from an airplane. Small airplanes and birds prefer fair weather and reluctantly compete for the airspace. A conflict between aircraft and birds is a real and growing problem - about 60,000 bird strikes to U.S. aircraft were reported to the FAA from 1990 to 2003, and perhaps four times that many went unreported [1]. A 12-pound Canada goose struck by a 150-mph aircraft generates the force of a 1,000-pound weight dropped from a height of 10 feet [2]. Damage to aircraft is estimated at \$400 million per year, and up to 400 (human) deaths have been

blamed on collisions with birds [1]. It is a natural wish that clear air surveillance radars have capabilities to detect birds, to detect small aircraft and to warn amateur pilots to avoid space occupied by birds.

Birds and aircraft produce substantially different spectral signatures even when these signatures are characterized by powers with low signal to noise ratios [3]–[5]. The spectrum of a resolution volume with a large bird in clear air can be visualized as a peak(s) from bird(s), and a peak from wind, both superimposed on a noise floor. The spectrum of a small airplane with propellers consists of a peak from the airplane, a possible peak from wind, and frequency modulated replicas or peaks from moving parts of the airplane, all superimposed on the noise floor. This signal spectrum appears to have a higher floor when compared to a resolution volume with no airplane present. Our method for airplane detection is based on estimating the inherent spectral floor for each resolution volume. We refer to this floor as the *noise map*. We utilize information from the noise map with two goals: (1) to improve detection of weak echoes in clear air (not addressed here), and (2) to provide aircraft detection. In current radar applications noise is considered to be a single value that is applied to the entire 360° azimuthal range of a given elevation [6]. We show that spectral noise level changes for resolution volumes with ground clutter and aircraft. We consider only ranges beyond 20 km from the radar to avoid echoes from ground clutter detected through the main and/or side lobes at low elevation angle of the radar beam. Our proposed method can even pinpoint an airplane if it has return power insufficient for detection in the current reflectivity display. Our presented method requires a sufficient number of pulses/samples for spectral processing [3], [5]. We demonstrate our method using time-series data collected in Norman Oklahoma in spring 2007 in clear air conditions.

## 2. RADAR SET UP AND DATA COLLECTION

Time-series data were collected with the research S-band Doppler radar (KOUN) which is maintained and operated by the National Oceanic and Atmospheric Administration/National Severe Storm Laboratory

(NOAA/NSSL) in Norman, Oklahoma. Data are collected in clear air and at elevation  $0.5^\circ$  on March 6, 2007 at 3 pm (20 UT). Radar antenna scanned  $360^\circ$  with a pulse repetition time PRT of  $780 \mu\text{s}$  and 128 pulses for spectral processing. Clear air and a light S-SW wind were reported on this day. Large birds (gulls and Canadian geese) were occasionally visible from the ground in the radar vicinity.

### 3. SPECTRAL ANALYSES OF ECHOES FROM AIRCRAFT

Radial at azimuth  $10^\circ$  is selected to illustrate differences in the noise floor in the resolution volumes with and without an aircraft. Fig. 1a shows power spectra  $S_h$  along the range between 20 and 45km from the radar. These are unprocessed spectra with original ground clutter and noise. The power is shown in logarithmic units. A contribution from the ground clutter is visible at  $0\text{ms}^{-1}$  and at ranges from 20 to 30km. A path produced by wind blown scatterers. Point scatterers whose echoes appear as dark blobs in Fig. 1a are birds. A dark line at 34km is the airplane spectrum with raised spectral floor. The shape of the airplane spectrum from 34km is shown in Fig. 1b together with a spectrum from clear air at 28km. The wind peak is at  $10\text{ms}^{-1}$  and the noise floor is at about  $-80 \text{ dB}$ . The airplane peak is at  $-7\text{ms}^{-1}$ . The noise floor in the airplane spectrum is at about  $-60 \text{ dB}$ ; that is 20 dB above the spectral floor of clear air. This increase in floor height is due to the modulations in the return caused by the moving propellers [7]. The total power from a resolution volume is a sum of all spectral coefficients scaled by the number of spectral coefficients. Clearly the contribution to the total power from the airplane or clear air in this case is insignificant. Neither of these signals is detectable with standard processing techniques due to the low signal to noise ratio.

There is nothing special about the selected radial shown in Fig. 1. A similar scenario occurs in other resolution volumes containing airplanes with propellers. Fig. 2 depicts spectra in azimuth locations of  $44^\circ$ ,  $59^\circ$  and  $333^\circ$  for ranges between 20 and 117km. The range locations containing aircraft can be easily recognized by the elevated spectral floor that appears as a dark vertical line in each example. The shape of each airplane spectrum is shown to the right from the corresponding spectral field in range; see Fig. 2a, b, c for ranges 87km, 61km, and 34km respectively.

### 3. TECHNIQUE

Spectral noise can be estimated from the rank order statistics on spectral coefficients of each resolution volume. The noise map is a collection of estimated levels of spectral noise. To obtain the noise map and simultaneously compute reflectivity, we perform the following steps for each range location of the recorded time-series data: (1) A Fourier

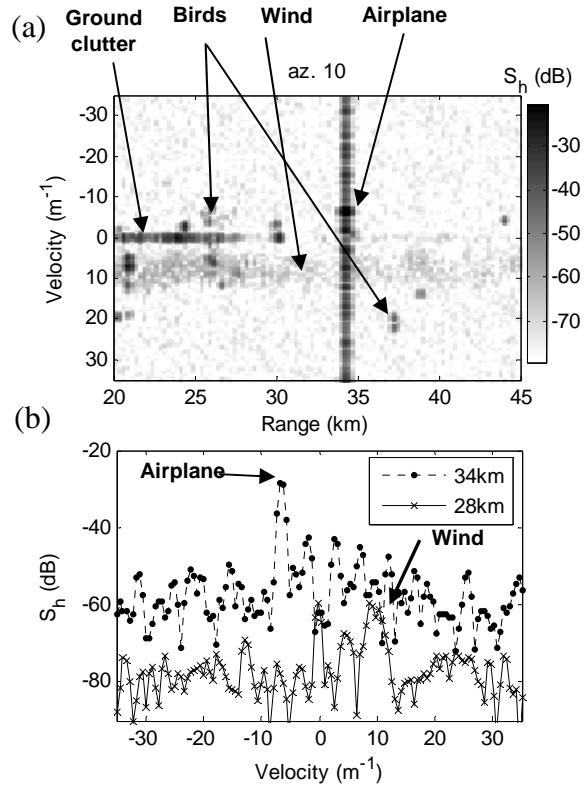


Fig. 1. Example illustrating airplane echo and its elevated level of spectral noise (a) spectra along range (b) spectra of resolution volumes with and without airplane as indicated.

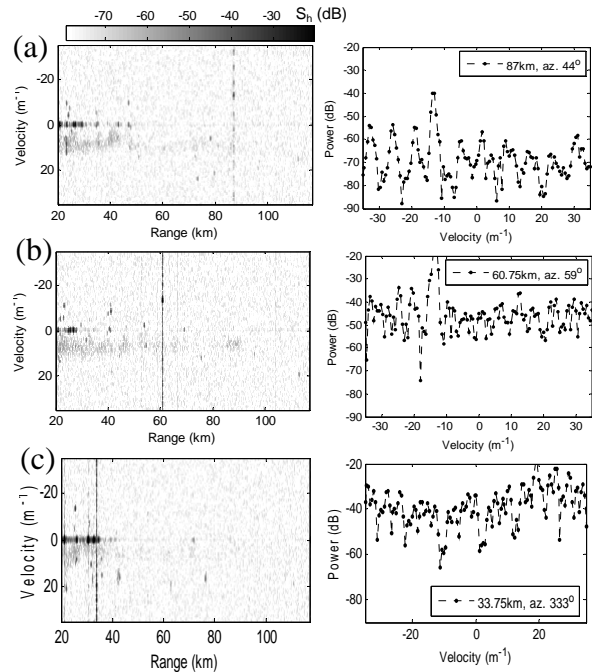


Fig. 2. Examples of spectra with aircraft: (a) in azimuth  $44^\circ$  and at range 87 km; (b)  $59^\circ$  and at 61 km, (c)  $333^\circ$  and 34 km. Aircraft in each radial is indicated with an arrow.

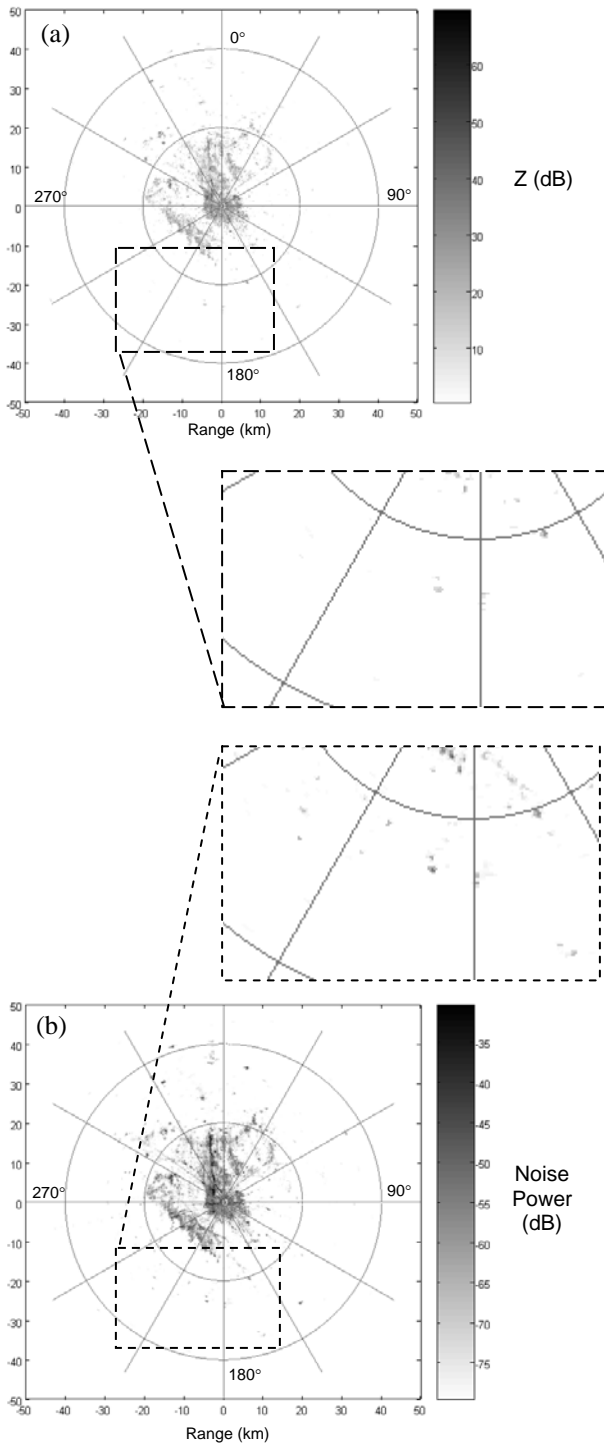


Fig. 3. Airplane signatures emerge in clear air display of (a) reflectivity, and (b) map of spectral noise level. This data are from March 6, 2007 at 3 pm, with 128 samples for spectral analyses.

analysis is used to obtain the power spectral density from the echo voltage multiplied by a window function (we use the Blackman window) [3], [5]; (2) Spectral coefficients are sorted in ascending order of their powers; (3) the noise level is estimated as a mean value of the lower half of ordered spectral coefficients and recorded in a map; (4) the power is adjusted relative to the noise level (PSD is shifted such that noise is at 0 dB) for ground clutter suppression and the reflectivity estimation.

#### 4. SPECTRAL NOISE LEVEL

Reflectivity  $Z$  shown in figure Fig. 3a reveals a number of point echoes at ranges beyond 20 km and the ground clutter residuals within 20 km range ring. Many of the points with high powers are from airplanes. Others are from radio towers and birds. The noise map shown in Fig. 3b exposes point echoes from moving scatterers whose spectral floor level is elevated. At close ranges the altitude of the center of the radar beam is low. Consequently the echoes exposed by the noise map close to the radar are mainly from the traffic detected through main or side lobes of the radar beam. As the center of the radar beam reaches sufficient altitude, the noise map exposes aircraft. Some of these aircraft are not visible in the reflectivity map (Fig. 3a) because the weak powers of their echoes cannot be displayed with presented color scale. The zoomed portions of Figs. 3a, 3b show many point targets detected with the noise map.

Another example (Fig.4) exposes echoes detected within the section of atmosphere between 320 m and 440 m altitude (30 km and 40 km in range), and between  $0^\circ$  and  $150^\circ$  azimuth. The maps of noise level, reflectivity with filtered ground clutter, and the ground clutter are shown in Figs. 4a, 4b, and 4c respectively. We do not use polar coordinates in these examples for an easier comparison of the fields presented in Figs. 4a, 4b and 4c. A more sensitive color scale is used in these examples to expose all echoes that have signatures different from the background (adjacent locations). The reflectivity field (Fig. 4b) exposes point echoes caused by aircraft, birds, and the residuals of ground clutter, detected through main and side lobes. The ground clutter map (Fig. 4c) shows locations of elevated terrain and non-moving structures on the ground. The noise level map (Fig. 4a) depicts several point targets that are also visible on the reflectivity field. However, in the reflectivity field these point targets do not stand out due to the presence of other point targets. The other point targets are birds and residuals from ground towers. The noise map shows aircraft clearly and so the map can be used to track the aircraft.

For reference we show the polarimetric variables for the section of atmosphere depicted in Fig. 4. The reflectivity, differential reflectivity between horizontal and vertical channels of the dual polarization radar, co-polar correlation coefficient, and differential phase are shown in Figs. 5a, 5b, 5c, and 5d respectively [3]. Presented polarimetric fields certainly do not bring clarity for the

airplane identification and/or detection. Locating the aircraft from the polarimetric fields would require a complex classification scheme for distinguishing all detected scatterers, such as birds, aircraft, insect, and/or their combinations.

### 5. CONCLUSION

A map of adaptively computed spectral floor pinpoints locations with airplanes and can be used for detecting and distinguishing small airplanes with propellers from birds and towers.

### 6. REFERENCES

[1] T. Cole, "Bird strikes a growing concern...as spring gets everyone flying," *Aviation Publishing Group*,

2005. [www.avweb.com/eletter/archives/avflash/214-full.html#186949](http://www.avweb.com/eletter/archives/avflash/214-full.html#186949).

[2] Bird Strike Committee USA, <http://www.birdstrike.org>, 2006.  
 [3] R. J. Doviak and D. S. Zrnic, *Doppler Radar and Weather Observations*, Academic Press, 1985.  
 [4] G. W. Stimson, 1998: *Introduction to Airborne radar*, SciTech Publishing Inc.  
 [5] M. H. Hayes, *Statistical Digital Signal Processing and Modeling*. John Wiley & Sons, 1996.  
 [6] U.S. Department of Commerce/NOAA, *Federal meteorological handbook #11: Doppler radar meteorological observations. Part C. WSR-88D products and algorithms*, FCM-H11C-2006.  
 [7] S. Bachmann, V. DeBrunner, D. Zrnic, and M. Yeary, "Techniques for detection and tracking airplanes using weather radar WSR-88D", *Proc. 38th Asilomar Conference*, IEEE, Pacific Grove, CA, USA, 1461, 2004.

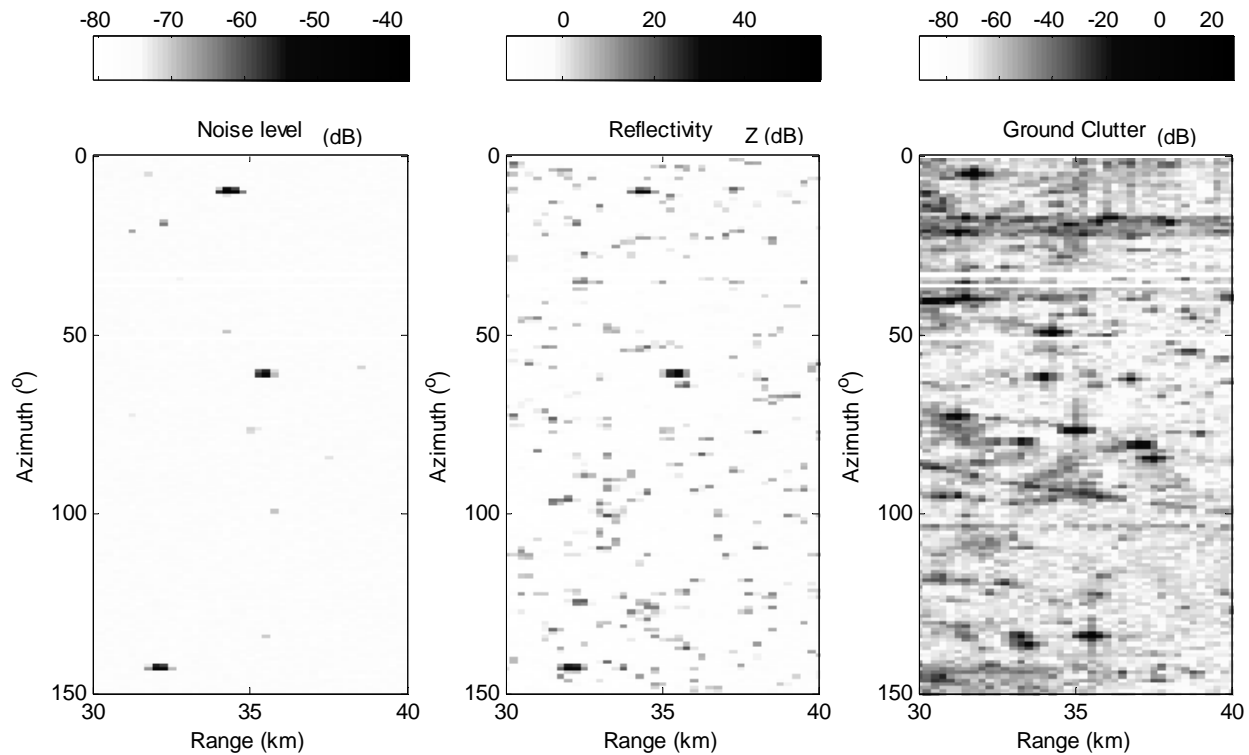


Fig. 4. Echoes detected within the section of atmosphere between 320 m and 440 m altitude (30 km and 40 km in range): (a) spectral noise level with revealed aircraft positions; (b) reflectivity with aircraft, birds and ground clutter residuals; (c) ground clutter with exposed towers, road structures, buildings, and terrain features. This data are from March 6, 2007 at 3 pm, with 128 samples for spectral analyses.

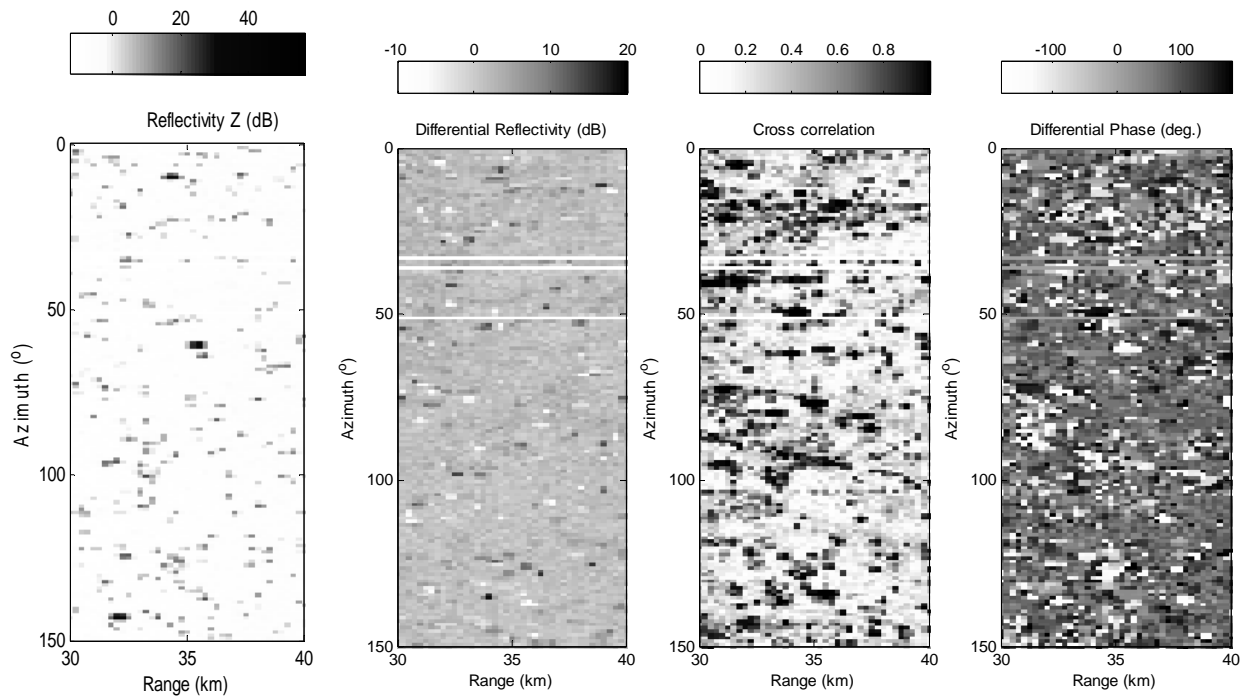


Fig. 5. Echoes detected within the section of atmosphere between 320 m and 440 m altitude (30 km and 40 km in range): (a) reflectivity with aircraft, birds and ground clutter residuals; (b) differential reflectivity between horizontal and vertical channels (c) co-polar correlation coefficient, and (d) differential phase. This data are from March 6, 2007 at 3 pm, with 128 samples for spectral analyses.